Inorg. Chem. **2002**, *41*, 5733–5743

Six-Coordinate Co^{2+} with H_2O and NH_3 Ligands: Which Spin State Is More Stable?

Ann M. Schmiedekamp*,†

Penn State University, Abington College, 1600 Woodland Road, Abington, Pennsylvania 19001

M. Dominic Ryan*,‡

GlaxoSmithKline, 706 Swedeland Road, King of Prussia, Pennsylvania 19406

Robert J. Deeth

Department of Chemistry, University of Warwick, Coventry CV4 7AL, U.K.

Received June 13, 2002

Octahedral, six-coordinate Co^{2+} can exist in two spin states. For biological ligands, H_2O and NH_3, the most stable spin state is high spin ($S = {}^3/_2$). The difference in energy between high and low spin is dependent upon the ligand mix and coordination stereochemistry. High spin optimized geometries for these model compounds give structures close to octahedral symmetry. Low spin permits significant Jahn–Teller distortion. H_2O ligands preferentially assume axial positions. Continuum solvent has a greater effect on low spin Co^{2+}, and it reduces the energy difference between the two spin states. For some ligand combinations optimized in the presence of solvent, there is no significant difference in energy between spin states.

Transition metals are at the core of the catalytic function of many metalloproteins. The theoretical simulation of such large systems typically requires an empirical method when high throughput is a priority. There are several approaches to treating transition metal environments in a molecular mechanics framework, or a coupled QM/MM method.[1] A common difficulty faced by all methods, including ab initio HF or DFT, is the need to assign a spin state to the metal center. The open d shell of transition metals such as d^7 Co^{2+} splits into two orbital manifolds in an octahedral environment: the higher energy e_g and lower energy t_{2g} states. Thus, Co^{2+} may take on one of two electronic states, a low spin $t_{2g}^6e_g^1$ state with one unpaired electron ($S = {}^1/_2$) and high spin $t_{2g}^5e_g^2$ with three unpaired electrons ($S = {}^3/_2$). The relative energy of the high spin and low spin configurations depends on the octahedral field strength, and therefore on the nature of the ligands. Ligands that are relevant to biological systems, such as water, ammonia, carboxylate, and imidazole, are approximately in the middle of the spectroscopic series[2] indicating that high spin is more likely, but not assured.

Co in the +2 oxidation state has been the subject of a small number of DFT calculations. While a few of these studies have been for two- or three-coordinated Co^{2+},[3] there are others that investigate Co for coordinations of 4−6. A study of $[Co(bipyr)_3]^{2+}$ with three bipodal groups included a brief DFT investigation on the structure at the X-ray geometry in three different oxidation states.[4] Tetrahedral coordination in Co^{2+} has been investigated for Co(ethylsulfanyl) porphyrazinato.[5] Agreement of Co−ligand bonds with

* To whom correspondence should be addressed. E-mail: ams@psu.edu (A.M.S.); dryan@mpi.com (M.D.R).

† Work performed at GlaxoSmithKline while on sabbatical leave from Penn State University.

‡ Present address, Millennium Pharmaceuticals, 75 Sidney Street, Cambridge, MA 01239.

(1) Maseras, F.; Morokuma, K. *J. Comput. Chem.* **1995**, *16*, 1170.

(2) Shriver, D. F.; Atkins, P.; Langford, C. H. *Inorganic Chemistry*; W. H. Freeman and Co.: New York, 1994; p 246.

(3) Baldridge, K. K.; O'Connor, J. M.; Chen, M. C.; Siegel, J. S. *J. Phys. Chem. A* **1999**, *103*, 10126−31. Margl, P.; Deng, L.; Ziegler, T. *Organometallics* **1999**, *18*, 5701−8. Braden, D. A.; Tyler, D. R. *J. Am. Chem. Soc.* **1998**, *120*, 942−947.

(4) Adam, K. R.; Anderson, P. A.; Astley, T.; Atkinson, I. M.; Charnock, J. M.; Garner, C. D.; Gulbis, J. M.; Hambley, T. W.; Hitchman, M. A.; Keene, F. R.; Tiekink, E. R. T. *J. Chem. Soc., Dalton Trans.* **1997**, *4*, 519−530.

(5) Ricciardi, G.; Rosa, A.; Ciofini, I.; Bencini, A. *Inorg. Chem.* **1999**, *38*, 1422−31.

10.1021/ic0257930 CCC: $22.00
Published on Web 09/28/2002

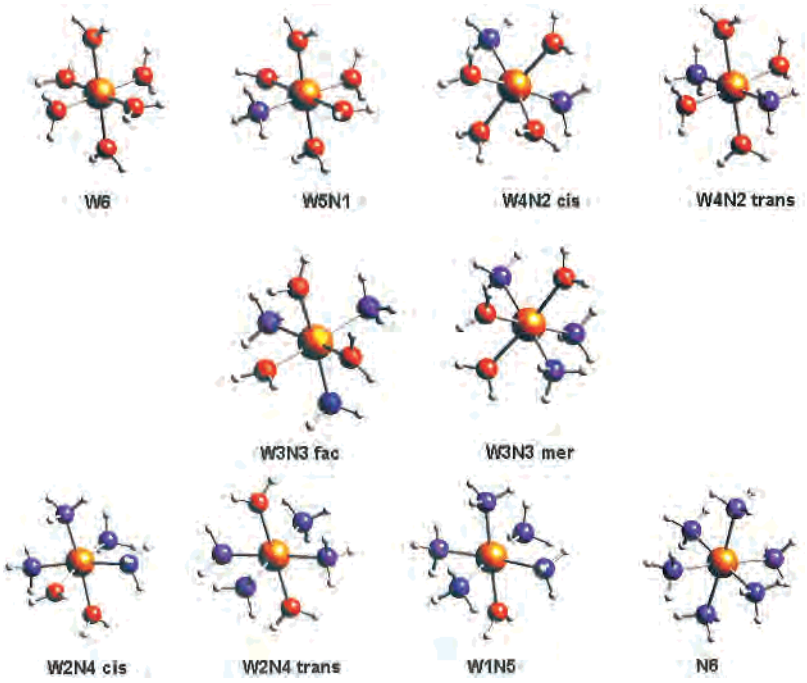

Figure 1. Model structures investigated.

EXAFS data was achieved in DFT geometry optimized calculations on tetrahedral cobalt substituted aluminophosphates in the +2 oxidation state.[6] These calculations also predicted that the most stable spin state is quartet (or high spin state) for the +2 oxidation state. Agreement with experimental data was achieved by fixing termination ligands on model compounds where molecular symmetry became distorted because of electrostatic attractions. Good agreement with crystal structure Co−O bond lengths has also been reported for DFT calculations on Co^{2+}(acacen)(pyridine) and Co^{2+}(salen)(pyridine) complexes.[7] In some of these systems, the low spin state ($S = {}^1/_2$) was found to be slightly more stable than the quartet state ($S = {}^3/_2$). The study of Co^{2+} bound to biologic ligands, in particular H_2O and NH_3, has not been reported in the literature.

This study seeks to compare the relative energies of high and low spin configurations of Co in the +2 oxidation state when bound to ligands NH_3 and H_2O (abbreviated herein as N and W, respectively). All combinations and isomers were studied in order to determine if the number or coordination stereochemistry of ligands would change the spin state of Co^{2+}. The structures investigated were $[Co(H_2O)_{6-n}(NH_3)_n]^{2+}$, $n = 0-6$ (Figure 1). An abbreviated nomenclature for these model compounds has been assigned as follows: W6, W5N1, W4N2cis, W4N2trans, W3N3fac (facial isomer), W3N3mer (meridional isomer), W2N4trans, W2N4cis, W1N5, and N6.

Computational Methods

For each of the model compounds, optimized geometries were obtained for both the low and high spin states using Jaguar 3.5 and 4.0.[8] The B3LYP functional[9] was employed throughout in conjunction with the LACVP** effective core potential basis set[10] for Co and 6-31G** bases[11] for all other atoms. During the SCF convergence, calculations were performed using a "fine" grid and "accurate" cutoffs. Precision was tested by using "ultrafine" cutoffs, and this did not change the energy more than 3×10^{-5} hartree. The energy convergence criterion was 5×10^{-5} hartree, and the density convergence criterion (root-mean-square change in density matrix elements) was 5×10^{-6}. Lowering either of these convergence criteria by a factor of 5 did not change the energy more than 1×10^{-4} hartree, nor did it change the energy difference between low and high spin for W6 more than the 1×10^{-4} hartree. Calculations were carried out at both restricted open shell density functional theory (RODFT) as well as unrestricted (UDFT).

Geometries were fully optimized except for the low spin cases where it was possible for the H_2O ligands to detach and hydrogen bond to a neighboring H_2O ligand (W6, W5N1, W4N2 cis, W3N3 fac and mer, W2N4). In these cases, relevant O−Co−O angles and dihedrals were fixed to prevent such a migration during the optimization. Vibrational frequencies were calculated for many of the structures at both RODFT (restricted open shell density functional theory) and UDFT (unrestricted density functional theory). These vibrational frequencies were calculated analytically for RODFT, but for UDFT, the frequencies are obtained from numerical gradient computations**.** Table 1 shows the magnitude of imaginary frequencies which resulted from both RODFT and UDFT optimizations**.** Table 2 shows the imaginary frequencies resulting

(6) Henson, N. J.; Hay, P. J.; Redondo, A. *J. Phys. Chem. A* **2000**, *104*, 2423−31.
(7) Hensen, N. J.; Hay, P. J.; Redondo, A. *Inorg. Chem*. **1999**, *38*, 1618−26.
(8) *Jaguar 3.5*; Schrodinger, Inc.: Portland, OR, 1998.
(9) Becke, A. D. *J. Chem. Phys*. **1993**, *98*, 5648. Local exchange functional: Slater, J. C. *Quantum Theory of Molecules and Solids, Vol. 4: The Self-Consistent Field for Molecules and Solids*; McGraw-Hill: New York, 1974. Nonlocal gradient correction exchange functional: Becke, A. D. *Phys. Rev. A* **1988**, *38*, 3098. Local correlation functional: Vosko, S. H.; Wilk, L.; Nusair, M. *Can. J. Phys*. **1980,** *58*, 1200. Nonlocal correlation functional: Lee, C.; Yang, W.; Parr, R. G. *Phys. Rev. B*, **1988**, *37*, 785.
(10) Hay, P. J.; Wadt, W. R. *J. Chem. Phys*. **1985**, *82*, 299.
(11) Ditchfield, R.; Hehre, W. J.; Pople, J. A. *J. Chem. Phys*. **1971**, *54*, 724.

Table 1. Imaginary Frequencies in cm^{-1} (Gas Phase Calculations)

	S	RODFT			UDFT			
W6	$^3/_2$				−314	−236	−84	
W6	$^1/_2$				−244.6	−201	−136.5	−77.7
W5N1	$^3/_2$	none			−327			
W5N1	$^1/_2$				−66.1	−31.2		
W4N2trans	$^3/_2$	none			−255.3			
W4N2cis	$^3/_2$	−127.6			−17			
W4N2cis	$^1/_2$	−315						
W3N3fac	$^1/_2$	none						
W3N3mer	$^3/_2$	−60.55	−54.6		−329	−99.5		
W3N3mer	$^1/_2$	none			none			
W2N4cis	$^3/_2$	−19.1			−26.8			
W1N5	$^3/_2$	−25.2			−106	−79		
W1N5	$^1/_2$	−138.9						
N6	$^3/_2$	−485.8	−245.6	−99.3	−239	−69.7		
N6	$^1/_2$	−284	−263	−91.54	none			

Table 2. Comparison of Energy Differences among W6 Stationary States

Δenergy (kJ/mol):	0.00	0.17	2.30	1.42	0.17	0.17	0.17
	Imaginary Frequencies (cm^{-1})						
	−265	−27	−437	−495	−269	−269	−268
	−70		−346	−291	−29	−21	−29
	−23		−156	−75			
			−116	−54			

from RODFT repeated optimizations on W6 where the geometry was changed slightly to force the structure into a local minimum. For W6, no structures were found without at least some small magnitude imaginary frequencies, but the energy differences between these stationary states are negligible as Table 2 shows. Finite grid sizes used in the density functional calculation contribute to the difficulty of locating a stationary state with no imaginary frequencies. Calculations were repeated in order to test the accuracy of the DFT method. Replicate calculations of a given geometry reproduce the energy to within 10^{-4} hartree (less than 0.4 kJ/mol). While vibrational analysis results in nontrivial imaginary frequencies, repeated geometry optimizations produce structures having different vibrational modes with imaginary frequencies, yet essentially the same geometry. For instance, in Table 2, two of the stationary states listed for W6, $S = {}^3/_2$, one with a frequency of -437 cm^{-1} and the other with a frequency of -269 cm^{-1}, have negligible differences in Co−ligand bond lengths (within 0.005 Å). The table shows that the differences in energy between these states is 2.1 kJ/mol. Since the energy difference between these different structures is negligible, it indicates that such saddle points are unlikely to affect the results.

In UDFT calculations, spin contamination (Table 3) was assessed by a comparison of the expected difference between $S(S + 1)$ for the assigned spin state and the actual value of $\langle S^2 \rangle$ from the DFT calculations and found to be negligible.

RODFT calculations were repeated including a continuum solvation method whereby the van der Waals radius of each atom determines a cavity size and the solvent energy is evaluated by a Poisson Boltzmann solver.[12] Solvation calculations were done both as a single point at the gas phase optimized geometry and as a geometry optimization in the presence of water. The difference in energy between the optimized gas phase structure and the structure optimized in a continuum environment may be viewed as the energy stabilization due to solvent (ΔE_{stab}). The stabilization energy is $\Delta E_{stab} = E_{soln} - E_{gas}$ where E_{gas} is the total energy of the structure

Table 3. Difference between Ideal and Actual Spin (Spin Contamination)

	$\langle S^2 \rangle$	fractional difference of $\langle S^2 \rangle$ from $S(S + 1)$[a]
	High Spin	
W6	3.752	0.0005
W5N1	3.753	0.0008
W4N2cis	3.753	0.0008
W4N2trans	3.753	0.0008
W3N3mer	3.753	0.0008
W3N3fac	3.753	0.0008
W2N4cis	3.753	0.0008
W2N4trans	3.753	0.0008
W1N5	3.754	0.0011
N6	3.753	0.0008
	Low Spin	
W6	0.752	0.0027
W5N1	0.759	0.0120
W4N2cis	0.756	0.0080
W4N2trans	0.755	0.0067
W3N3mer	0.757	0.0093
W3N3fac	0.757	0.0093
W2N4cis	0.762	0.0160
W2N4trans	0.755	0.0067
W1N5	0.755	0.0067
N6	0.755	0.0067

[a] For high spin, $S = {}^3/_2$ so $S(S + 1) = 3.75$; for low spin, $S = {}^1/_2$, so $S(S + 1) = 0.75$.

in the gas phase and E_{soln} is the solution phase energy. Solution phase energy,[13] as opposed to the gas phase energy, is the appropriate energy of the system evaluated using a continuum solvation model. It is the sum of the total solute energy, total solvent energy, and cavity energy. The solvent energy is computed to be half of the nuclear−solvent and electron−solvent terms. The solute cavity energy is the energy attributed to making a cavity of the size necessary to accommodate the solute molecule. Solution phase energy, E_{soln}, may also be written as

$$E_{soln} = E_{totalqm} - (E_{electron-solv})/2 - (E_{nuclear-solv})/2 + E_{cavity}$$

where E_{qm} is the total quantum mechanical energy for the entirety of the molecule and solvent system, $E_{electron-solv}$ is the energy attributed to the electron solvent interaction, $E_{nuclear-solvent}$ is the energy attributed to the nuclear-solvent interaction, and E_{cavity} is the solute cavity energy.

Recently, the meaning of Kohn−Sham (KS) orbitals has been debated in the literature. Although density orbital energy values

(12) Tannor, D. J.; Marten, B.; Murphy, R.; Friesner, R. A.; Sitkoff, D.; Nichaolls, A.; Ringnalda, M.; Goddard, W. A., III; Honig, B. *J. Am Chem. Soc*. **1994**, *116*, 11875.

(13) Wright, J. R. *Jaguar User's Guide, Version 4.0*; Schrodinger, Inc.: Portland, OR, 2000; p 98−99.

Table 4. Low Spin ($S = {}^1/_2$) Co−Ligand Bond Lengths (Gas Phase and Solvent)

	Co−O1	Co−O2	Co−O3	Co−O4	Co−O5	Co−O6	Co−N1	Co−N2	Co−N3	Co−N4	Co−N5	Co−N6
W6	2.182[a]	2.181	2.037	2.037	1.960	1.960						
	0.027[b]	0.027	−0.047	−0.048	0.019	0.019						
W5N1	2.210	2.232	2.045	2.049	1.985							1.983
	−0.001	−0.026	−0.005	0.006	0.003							−0.008
W4N2cis	2.298	2.285	2.019		2.027					2.009		2.017
	−0.009	0.000	−0.004		0.005					−0.008		−0.014
W4N2trans	2.249	2.251	2.069	2.069							2.002	2.002
	−0.014	−0.018	−0.020	−0.020							−0.004	−0.005
W3N3mer	2.354	2.343	2.051							2.033	2.023	2.016
	−0.022	−0.029	−0.006							−0.011	−0.011	−0.003
W3N3fac	2.397		2.051		2.029			2.272		2.035		2.015
	−0.052		−0.013		−0.003			−0.004		−0.017		−0.008
W2N4cis	2.338				2.086			2.345	2.023	2.022		2.067
	0.011				−0.017			−0.028	−0.010	−0.001		−0.022
W2N4trans	2.382	2.383							2.039	2.040	2.039	2.040
	−0.005	−0.006							−0.014	−0.015	−0.013	−0.015
W1N5	2.475							2.358	2.043	2.042	2.062	2.062
	0.018							−0.026	−0.009	−0.008	−0.019	−0.020
N6							2.439	2.441	2.063	2.062	2.062	2.061
							−0.004	−0.008	0.000	0.002	0.001	0.005

[a] Bond lengths in angstroms. [b] Difference between bond length in solvent and in gas phase, $d_{solv} - d_{gas}$.

must be scaled linearly to estimate ionization potentials, Stowasser and Hoffmann[14] suggest that KS orbitals can provide a qualitative interpretation for chemical phenomena. Furthermore, Stowasser and Hoffmann show that the hybrid B3LYP, when compared to KS orbitals from BP86, have similar orbital energy differences. B3LYP density orbitals involving Co d and ligand p orbitals are studied in order to better understand the geometry and energy variations obtained in the calculations.

Results

I. Geometries. A. Low Spin Geometries. The low spin d^7 configuration is subject to a strong Jahn−Teller effect[15] which results in a large tetragonal elongation often leading to complete loss of the axial ligands. However, in the present calculations, the axial groups do not escape completely, and the optimized geometries display four short equatorial bonds and two long axial contacts giving complexes of approximately D_{4h} symmetry. Table 4 lists the Co−L bond lengths for low spin complexes paired as three sets of trans ligands. Ligands are listed in pairs (1,2), (3,4), and (5,6), with (1,2) being the designated axial pair. The axial positions are identified not only as the ligands having the longest bond lengths but also by their orbital participation. Axial ligands are the ligand pair with the highest p, d_{z^2} overlap in the e_g orbital. In all low spin cases, the ligand pair with the greatest p orbital contribution in the e_g orbital also has the longest cobalt−ligand bond length.

There is a notable difference between the symmetry of low spin N6 and W6. N6 has the expected tetragonal coordination of four equal equatorial bonds at 2.06 Å and two long axial contacts at 2.44 Å. However, low spin W6 has rhombic symmetry (D_{2h}) with two significantly different equatorial bond lengths of 1.96 and 2.04 Å. Rhombic symmetry is also characteristic of high spin W6 both in the experimental crystal structures[16] (Table 5) and theoretically (vide infra). The difference between W6 and N6 arises from a combination of steric and electronic effects. Sterically, the H atoms on the four equatorial NH_3 ligands can pack such that the symmetry of the $[Co(NH_3)_4]^{2+}$ fragment is $\sim D_{2d}$ and all four groups are equivalent. In contrast, the H atoms from one pair of water ligands lie parallel to the equatorial plane of W6 while those on the other two are perpendicular. The W6 ligand environment is also sterically and electronically different from N6 because of the intramolecular hydrogen bonding pattern.

In W6, the orientation of the planes of the ligands ensures that each pair of trans-related ligands interacts with a single component of the d−π orbitals (i.e., the "t_{2g}" functions in O_h symmetry). This arises because each water molecule binds

Table 5. Comparison of W6 Bonds with Experiment

ref	Co−O1[a]	Co−O2	Co−O3	Co−O4	Co−O5	Co−O6
16a	2.115	2.115	2.097	2.097	2.040	2.040
16b	2.129	2.129	2.073	2.073	2.049	2.049
16c	2.118	2.118	2.113	2.113	2.087	2.087
16d	2.105	2.105	2.085	2.085	2.062	2.062
16e	2.086	2.086	2.085	2.085	2.051	2.051
16f	2.120	2.120	2.066	2.066	2.058	2.058
16g	2.110	2.110	2.052	2.052	2.045	2.045
16h	2.103	2.103	2.087	2.087	2.053	2.053
16i	2.119	2.119	2.078	2.078	2.046	2.046
16j	2.158	2.104	2.097	2.091	2.054	2.053
16k	2.116	2.116	2.105	2.105	2.051	2.051
average exptl value	2.116	2.111	2.085	2.085	2.054	2.054
high spin optimized geometry	2.123	2.124	2.119	2.119	2.119	2.119
difference from expt	0.007	0.013	0.034	0.034	0.065	0.065
low spin optimized geometry	2.182	2.181	2.037	2.037	1.96	1.96
difference from expt	0.066	0.070	−0.048	−0.048	−0.094	−0.094
high spin optimized geometry with solvent	2.193	2.193	2.005	2.004	1.965	1.965
difference from expt	0.077	0.082	−0.080	−0.080	−0.089	−0.089
low spin optimized geometry with solvent	2.209	2.208	1.990	1.989	1.979	1.979
difference from expt	0.092	0.097	−0.095	−0.096	−0.076	−0.075

[a] Bond lengths in angstroms.

(14) Stowasser, R.; Hoffmann, R. *J. Am. Chem. Soc*. **1999**, *121*, 3414−3420.
(15) Shriver, D. F.; Atkins, P.; Langford, C. H. *Inorganic Chemistry*; W. H. Freeman and Co.: New York, 1994; p 255.

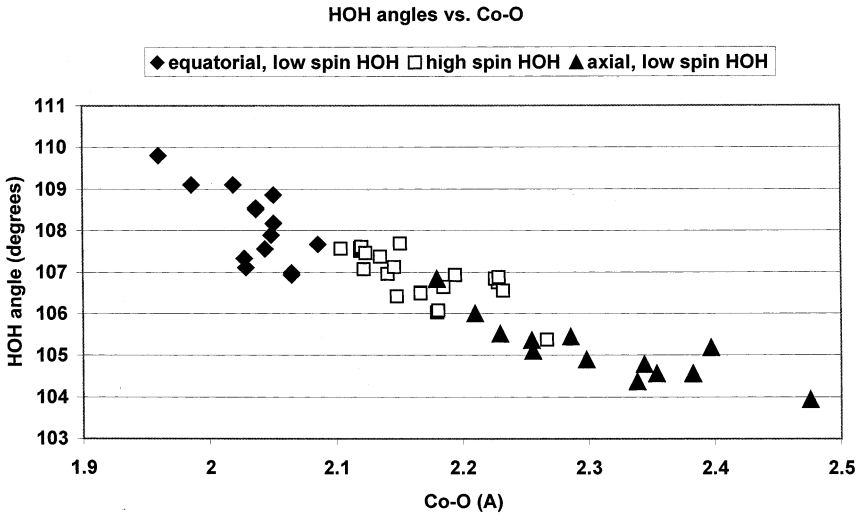

Figure 2. HOH bond angles vs Co−O bond lengths for all model compounds.

the water with the hydrogens directed away from the metal and oxygen lone pairs, perpendicular to the ligand plane, available for a metal−ligand π interaction. The HOH angles are identical in each trans pair, demonstrating that similar orbital interactions are active for each ligand of the pair. In Figure 2, HOH angles in water ligands are plotted versus Co−O bond lengths for all model optimized structures. For the longest Co−O bonds, corresponding to the axial ligands, the water HOH angle is the same as the gas phase experimental value 104.5°,[17] confirming the sp^3 character of the ligand. The experimental value is also well reproduced by a gas phase optimization of H_2O using the B3LYP functional (103.95°). Figure 2 shows that, as the Co−O distance decreases, the HOH angle increases, and the water oxygens take on slightly more sp^2 character, though still distant from a full sp^2 HOH angle of 120°. The increase of sp^2 character is expected intuitively if the decrease in distance increases the overlap between O p and Co d orbitals, thus raising the energy of the oxygen lone pair. Energy of the lone pair would be increased because one of the O lone pairs would be perpendicular to the plane of the HOH and Co atoms. As a result, the oxygen atom has an increased s component evidenced by the increased HOH bond angle. NBO analysis shows that axial O lone pairs have 3% more s character for cases of shorter Co−O bonds.

The effect in NH_3 is smaller as shown in Figure 3. Ligands with the longest Co−N distance also have more compressed HNH angles. For H_2O ligands, the more compressed H bond angle brings the ligand structure closer to the gas phase result, but for NH_3 ligands, the compression of the H bond angle pulls the value further from the gas phase geometry both experimentally (106.5°)[17] and as determined by B3LYP calculations (106.1°). The magnitude of this effect is, however, only spread over a range of 3°, and it indicates a lack of the π interaction seen with H_2O. The slight compression in NH_3 ligands with longer Co−N distances is perhaps due to the influence of the d_{z^2} orbital density, because those ligands are all axial, whereas the equatorial ligands all have HNH bond angles much closer to the gas phase values.

Differences in N6 and W6 are also seen in the Co d orbital compositions. Table 6 lists the characteristics of the low spin Co d and ligand p orbitals in W6 and N6. As noted previously, the longest two pairs of Co−O bonds are associated with the antibonding e_g orbital. The large difference in the two equatorial trans pair bond lengths is related to the destroyed degeneracy of the t_{2g} antibonding orbitals. Only anti- and nonbonding orbitals are listed in Table 6, but the calculations show that the longest bonds, d(Co−O) = 2.18 Å, of ligands 1 and 2, are found in the least stable Co d,p bonding (t_{2g}) orbital. The most stable bonding orbital is for the ligand pair with the shortest bond length, d(Co−O) = 1.96 Å, in ligands 5 and 6.

In a ligand field context based on either the angular overlap model[18] (AOM) or the cellular ligand field (CLF) model,[19] a saturated nitrogen donor such as NH_3 has no π-bonding capability, and hence, the d_{xy}, d_{yz}, and d_{xz} orbitals in N6 are expected to be nonbonding while the d_{z^2} and $d_{x^2-y^2}$ orbitals are antibonding. Table 6 shows that the t_{2g} valence Co orbitals are completely nonbonding with no ligand participation. The ground state of the octahedral $[Co(NH_3)_6]^{2+}$ precursor is formally ^2E_g and thus parallels the comparable d^9 Cu^{2+} species. To first order, the Jahn−Teller distortion

(16) (a) Viossat, B.; Khodadad, P.; Rodier, N. *Bull. Soc. Chim. Fr.* **1981**, 69−71. (b) Nassimbeni, L. R.; Percy, G. C.; Rodgers, R. L. *Acta Crystallogr., Sect. B* **1976**, *32*, 1252. (c) Zviedre, I.; Fundamenskii, V. S.; Kolesnikova, G. P. *Koord. Khim.* **1984**, *10*, 1408. (d) Brach, I.; Roziere, J.; Anselment, B.; Peters, K. *Acta Crystallogr., Sect. C* **1987**, *43*, 458. (e) Ganesh, V.; Seshasayee, M.; Aravamudan, G.; Heijdenrijk, D.; Schenk, H. *Acta Crystallogr., Sect. C* **1990**, *46*, 949. (f) McCandlish, E. F. K.; Michael, T. K.; Neal, J. A.; Lingafelter, E. C.; Rose, N. J. *Inorg. Chem.* **1978**, *17*, 1383. (g) Wolodkiewicz, W.; Brzyska, W.; Glowiak, T. *Pol. J. Chem.* **1996**, *70*, 409. (h) Kepert, C.; Hesek, J. D.; Beer, P. D.; Rosseinsky, M. J. *Angew. Chem., Int. Ed.* **1998**, *37*, 3158. (i) Perez, J. M. G.; Gutierrez, J. N.; Dung, N. H.; Voissat, B.; Busnot, A.; Wintenberger, M. *Inorg. Chim. Acta* **1991**, *184*, 243. (j) Podlaha, J.; Podlahova, J.; Stepnicka, P.; Rieder, M. *Polyhedron* **1994**, *13*, 2847. (k) Porai-Koshits, M. A.; Antsyshkina, A. S.; Shkol'nikova, L. M.; Sadikov, G. G.; Davidovich, R. L. *Koord. Khim.* **1995**, *21*, 311.
(17) *CRC Handbook of Chemistry and Physics*, 80th ed.; Lide, D. R., Ed.; CRC Press: New York, 1999.
(18) Schaeffer, C. E.; Jorgensen, C. K. *Mol. Phys.* **1965**, *9*, 401.
(19) Deeth, R. J.; Gerloch, M. *J. Chem. Soc., Dalton Trans.* **1986**, 1531−1534.

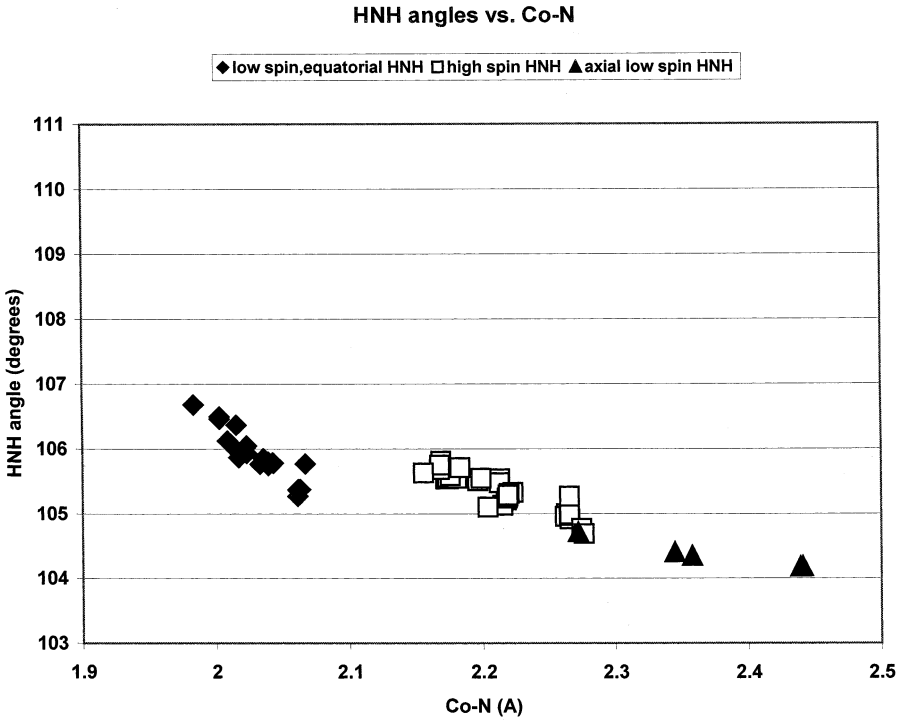

Figure 3. HNH angles vs Co−N bond lengths for all model compounds.

Table 6. Low Spin W6 and N6 Co d and p Orbitals Involved in Ligand Bonding

W6						N6					
bond length	ligand	α orbital symmetry	α orbital energy (hartree)	β orbital symmetry	β orbital energy (hartree)	bond length	ligands	α orbital symmetry	α orbital energy (hartree)	β orbital symmetry	β orbital energy (hartree)
					d,p Antibonding						
	O(1,2) and O(3,4)	e_g	−0.581	e_g		2.40	N(1,2)	e_g	−0.501	e_g	
					d,p Nonbonding						
2.04	O(3,4)	t_{2g}	−0.587	t_{2g}	−0.574			t_{2g}	−0.544	t_{2g}	−0.527
2.18	O(1,2)	t_{2g}	−0.604	t_{2g}	−0.589			t_{2g}	−0.544	t_{2g}	−0.527
1.96	O(5,6)	t_{2g}	−0.621	t_{2g}	−0.599			t_{2g}	−0.574	t_{2g}	−0.546

favors neither a compressed nor an elongated geometry. However, second order influences such as vibrational anharmonicity, d−s mixing and higher order contributions to the Jahn−Teller electronic energy favor an axial elongation. For N6, the axial Co−N distances are nearly 0.4 Å longer than the equatorial contacts.

In mixed ligand model compounds, the structures show intermediate characteristics between N6 and W6 both in orbitals (Figure 4) and in geometry (Table 4). In fact, as NH_3 replaces H_2O in W6, a gradual shift from N6 to W6 geometries is seen. In the equatorial plane, the Co−N length increases as more waters are replaced. Because NH_3 is a better donor than H_2O, the Co−N bond strength is enhanced at the expense of the Co−O interaction. The more Co−N bonds, the greater the mutual competition and the longer the average Co−N distance. Hence, the equatorial Co−N distance increases from 1.983 Å in W5N1 to 2.062 Å in N6. Axial bond lengths have somewhat different trends. Where a choice is possible, water is always found to occupy the axial position. Inasmuch as H_2O is a weaker donor ligand, it is energetically better to have H_2O in an axial position, interacting with the antibonding d_{z^2} orbital, than the stronger donor NH_3. As the number of NH_3 groups increases in the molecule, both the Co−O and Co−N axial bond lengths increase. The molecular symmetry also shows a gradual transition from rhombic W6 to tetragonal N6 as NH_3 ligands replace H_2O.

Additional symmetry breaking is evident in deviations of ligand−metal−ligand bond angles from ideal octahedral geometries because of a combination of steric and electrostatic factors such as crowding of NH_3 ligands or hydrogen bonding between H_2O and other ligands. Further calculations to reveal the energy surface associated with angle deformation suggest that the potential energy surface is very flat.[20]

B. High Spin Geometries. With respect to the Co−ligand bonds, the high spin complexes exhibit more regular "octahedral" symmetry, with much smaller deviations between axial and equatorial ligand sets. Indeed, the assignment of bonds as either axial or equatorial is ambiguous in many cases. The ground state of an octahedral high spin d^7 complex is $^4T_{1g}$ which is also formally Jahn−Teller active although the distortions are smaller because the degeneracy is associ-

(20) Unpublished results.

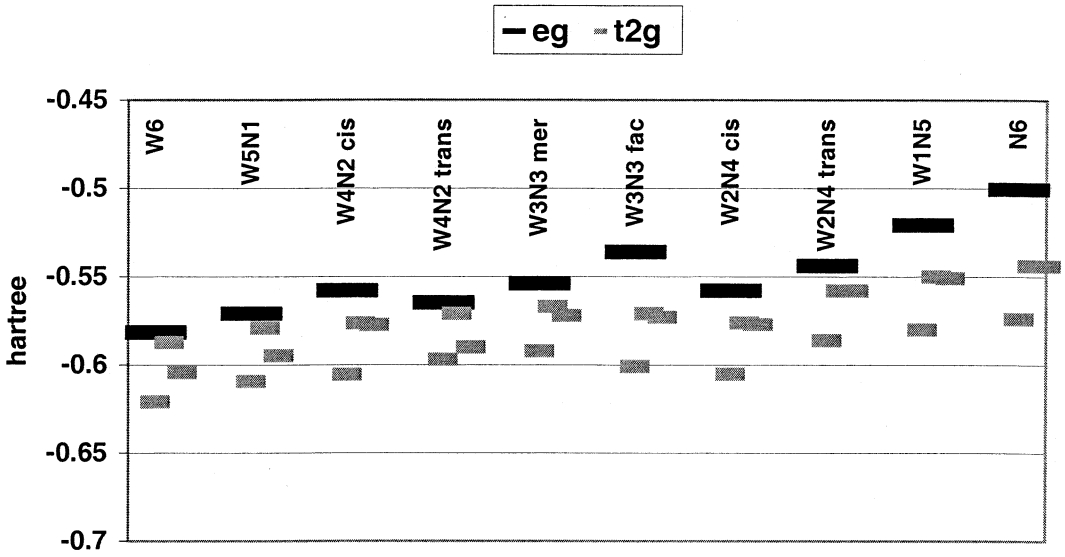

Figure 4. Antibonding Co d orbitals for $S = {}^1/_2$ (low spin).

Table 7. High Spin ($S = {}^3/_2$) Co−Ligand Bond Lengths (Gas Phase and Solvent)

	Co−O1	Co−O2	Co−O3	Co−O4	Co−O5	Co−O6	Co−N1	Co−N2	Co−N3	Co−N4	Co−N5	Co−N6
W6	2.12[a]	2.124	2.119	2.119	2.119	2.119						
	0.070[b]	0.069	−0.114	−0.115	−0.154	−0.154						
W5N1	2.151		2.141	2.145	2.135	2.147	2.156					
	0.010		−0.004	−0.012	0.005	−0.001	0.007					
W4N2cis	2.194		2.185		2.122	2.104		2.204		2.169		
	−0.008		−0.018		0.052	0.052		−0.044		−0.009		
W4N2trans			2.167	2.167	2.181	2.180	2.167	2.167				
			−0.007	−0.007	−0.018	−0.018	0.008	0.008				
W3N3mer			2.152		2.246	2.251	2.172	2.172		2.181		
			0.004		−0.027	−0.029	−0.002	0.001		−0.015		
W3N3fac	2.229		2.226		2.229			2.172		2.174		2.174
	−0.049		−0.026		−0.039			0.018		0.000		0.008
W2N4cis			2.271		2.234		2.224	2.199		2.216		2.195
			−0.036		−0.009		−0.007	−0.011		−0.022		−0.010
W2N4trans					2.213	2.213	2.219	2.219	2.219	2.219		
					−0.011	−0.009	−0.013	−0.011	−0.012	−0.012		
W1N5				2.209			2.274	2.276	2.217		2.213	2.213
				−0.027			−0.028	−0.028	−0.025		−0.015	−0.017
N6							2.263	2.265	2.262	2.265	2.266	2.265
							−0.023	−0.023	−0.018	−0.023	−0.023	−0.016

[a] Bond lengths in angstroms. [b] Difference between bond length in solvent and in gas phase, $d_{solv} - d_{gas}$.

ated with M−L π interactions. However, the vibronic coupling problem is far more complex than for the low spin ^2E_g case, and many different distortions are possible. As in the low spin cases, additional evidence is sought from the orbital participation to make an axial or equatorial assignment. The ligand pair involved in the d_{z^2} symmetry in an antibonding e_g orbital is designated as axial. Analysis of the orbital symmetries shows that axial assignments for high spin cases made on the basis of bond length are misleading because Jahn−Teller distortions are slight. Even orbital symmetry analysis is somewhat ambiguous on the assignment of axial ligands. Table 7 gives ligand bond lengths for high spin ($S = {}^3/_2$) Co^{2+} complexes. In W3N3mer, as well as W2N4trans and W4N2cis, O−O is the axial ligand pair while N−N is axial in the other structures. In W3N3fac, where there exist three trans pairs of N−O ligands, the difference between ligand pairs is not significant. In the HOMO and HOMO − 1 orbitals, the symmetries are identical but involve different ligand pairs, and the orbital energies are degenerate (Figure 5).

In contrast to the low spin homoleptic structure, high spin N6 has "octahedral" symmetry, inasmuch as all bond lengths are equal and all bonds are represented in the antibonding e_g orbitals. W6 exhibits a small but definite Jahn−Teller distortion with four equal equatorial Co−O bonds and two axial bonds, longer by 0.004 Å. Experimental crystal structures (Table 5) of compounds containing the $[Co(H_2O)_6]^{2+}$ complex give Co−O distances in good agreement with the present DFT results suggesting that the differences are real and a result of a Jahn−Teller effect. B3LYP optimized Co−O bond lengths are greater than the average experimental values by less than 0.06. B3LYP overestimates the Co−N distance by up to 0.1 Å.[21] Further, Table 7 shows that, for high spin, there is little difference between axial and equatorial bond lengths across all compounds and that

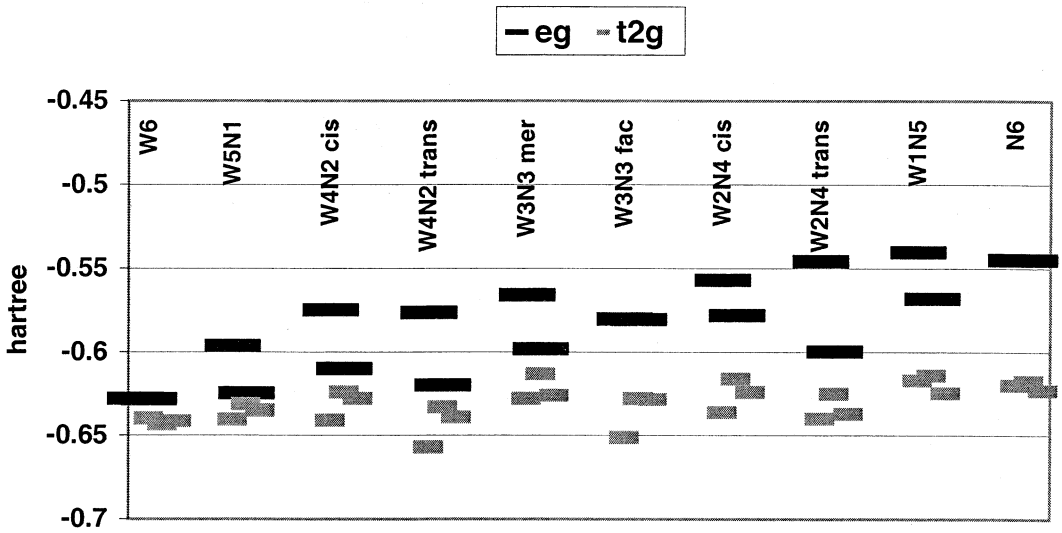

Figure 5. Antibonding Co d orbitals for $S = {}^3/_2$ (high spin).

Table 8. High Spin W6 and N6 Co d and p Orbitals Involved in Ligand Bonding

W6					N6				
ligand involved in orbital	α orbital symmetry	α orbital energy (hartree)	β orbital symmetry	β orbital energy (hartree)	ligands	α orbital symmetry	α orbital energy (hartree)	β orbital symmetry	β orbital energy (hartree)
				Antibonding					
Co−O axial	t_{2g}	−0.628			all ligands	e_g	−0.545		
Co−O eq	t_{2g}	−0.628			4 ligands	e_g	−0.545		
				Nonbonding					
Co−O eq	e_g	−0.640			all ligands	t_{2g}	−0.618		
Co−O axial	t_{2g}	−0.641	t_{2g}	−0.595	no ligands	$t_{2g} + e_g$	−0.620	t_{2g}	−0.554
Co−O eq	e_g	−0.642	e_g	−0.595	4 ligands	t_{2g}	−0.623	t_{2g}	−0.555

there is only a slight difference between Co−O and Co−N bond lengths. As in the low spin model compounds, Co−N bonds get longer as N ligands replace O ligands across the series, but in high spin, the differences in bond lengths are less pronounced.

For high spin, all geometries were completely optimized. Even though high spin geometries are much closer to octahedral symmetry, the L−Co−L ligand angles still deviate slightly from 90°, and the deviations, as in the low spin structures, appear to be driven by electrostatic attractions between the H_2O ligands.

C. High and Low Spin−Orbital Energies. An analysis of the Kohn−Sham molecular orbital energies provides some explanation for the geometry trends. Although both α- and β-spin−orbitals are available from the UDFT calculations, only the occupied α-spin−orbitals are plotted in Figures 4 and 5 because they represent the majority spin. The comparable functions with β-spin have virtually identical compositions and energy differences to those of their α-spin counterparts. Analysis of these (occupied) molecular orbital energies for low spin (Figure 4) shows the greatest symmetry in N6, where the original t_{2g} orbitals divide into two sets, axial and equatorial as described previously. Despite the AOM predictions, the three metal d_π orbitals are not degenerate because of electrostatic interactions implicit in the DFT calculation. These arise because the electron density distribution is asymmetric in the sense that to a first approximation there is formally one electron in d_{z^2} but $d_{x^2-y^2}$ is empty. Hence, the remaining d orbital lying in the *xy* plane, d_{xy}, is distinguished from those perpendicular to *xy*, d_{xz} and d_{yz}. For W6, there is the added complication of Co−O π interactions so all the d_π degeneracy is removed. The intermediate mixed ligand cases exhibit intermediate behavior. W5N1 is similar to W6, and so too is the antibonding orbital structure which shows no degeneracy in the t_{2g} orbitals. W1N5 and W2N4, on the other hand, possess two degenerate orbitals because the structures more closely approach that of N6.

The contrast between high spin W6 and N6 orbitals further emphasizes the nature of the metal−ligand bonding (Figure 5). N6 is essentially octahedral in geometry, and the orbitals correspond to the classic ligand field theory picture where the e_g and t_{2g} orbitals are degenerate. Every orbital shows delocalization over four or all six ligands (Table 8). The antibonding and nonbonding orbitals of N6 are of higher energy than the corresponding orbitals in W6 while the bonding t_{2g} orbitals are more stable, showing that NH_3 presents itself as a stronger ligand in both high and low spin states (vide supra). In W6, all five of the antibonding orbitals are essentially degenerate because their observed symmetries are mixtures of e_g and t_{2g}. This is to be contrasted with the

(21) 2.183 Å (BF_4 salt), 2.186 Å (PF_6), 2.113 Å (Cl), 2.170 Å (Cl): Newman, J. M.; Binns, M.; Hambley, T. W.; Freeman, H. C. *Inorg. Chem.* **1991**, *30*, 3499−3502.

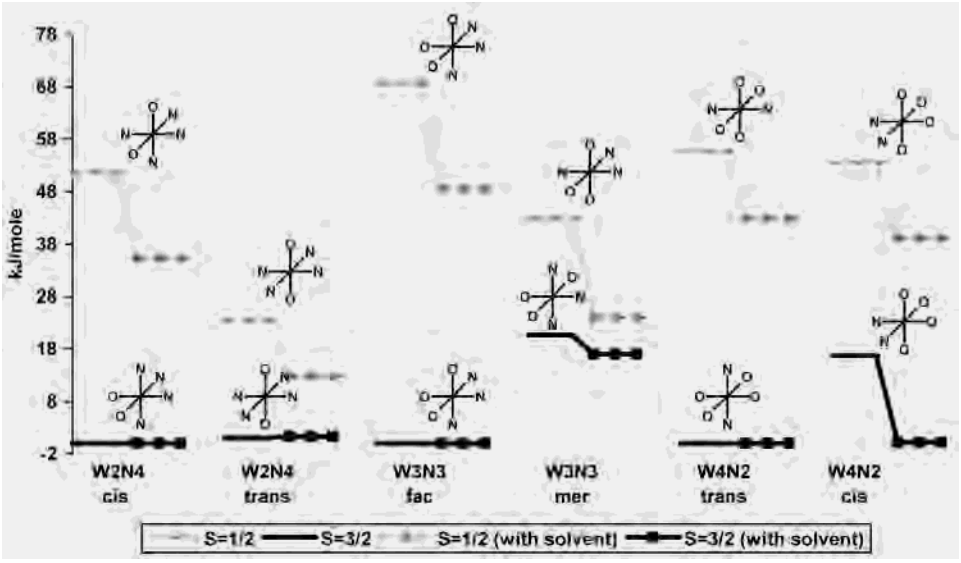

Figure 6. Comparison of isomer energies; structures are diagrammed immediately above the energy. Ligands oriented in the vertical direction are designated axial.

situation in N6 where the e_g orbitals are approximately 0.08 hartree higher than the t_{2g} orbitals. This too suggests that the orbital energies predict NH_3 to be the stronger of the two ligands.[22]

Table 7 shows that, for high spin, there is little difference between axial and equatorial bond lengths and that there is only a slight difference between Co−O and Co−N bond lengths. As in the low spin model compounds, Co−N bonds get longer as N ligands replace O ligands across the series, but in high spin, the differences in bond lengths are less pronounced. Figure 5 plots the energies of the mostly d based antibonding orbitals. In general, the "e_g" orbitals, d_{z^2} and $d_{x^2-y^2}$, increase in energy as NH_3 replaces H_2O. This is consistent with stronger Co−N than Co−O bonding. The t_{2g} orbital energies remain relatively constant for most of the mixed ligand high spin compounds; however, the 2-fold degeneracy is destroyed. The e_g orbitals are degenerate for only three cases, W6, W3N3fac, and N6. If one computes an estimate for Δ_{oct} based on the difference in these orbital energies, the net effect is to increase Δ_{oct} as NH_3 ligands are substituted for H_2O. An estimate for Δ_{oct} for N6 is approximately 17600 cm^{-1}, and for W3N3fac, 10970 cm^{-1}. The first value is in reasonable agreement with UV absorption observed for Co^{2+}.[23]

II. Energies. The absolute energies of all low spin or high spin complexes may be compared to determine which spin state is more stable. In addition, W3N3, W2N4, and W4N2 all have two structural isomers which permit calculating a relative energy for these pairs shown in Figure 6. In all cases, the lowest energy structure is high spin.

A. Low Spin Energies. In low spin, the presence of a H_2O ligand in the axial position is preferred energetically over the stronger donor ligand NH_3 when there is a choice between two different configurations. In Figure 6, the diagrams of isomer structures are depicted above their energies. In these diagrams, the vertical direction represents the *z* axis and therefore the axial direction. In each of the low spin ($S = {}^1/_2$) cases, the maximum number of O ligands appear in the axial direction. For example, W2N4 trans could have either two O ligands or two N ligands in an axial configuration, and axial O's are found. Cis W2N4 could have either two N's or one O and one N in an axial configuration, and the latter is found. Meridional W3N3 presents the choice of two O's axial, two N's axial, or one O and one N axial, but again, two O's are selected. Although not diagrammed in Figure 6, it is easy to visualize that W5N1 could have either two O's or one O and one N in an axial orientation, and the former is seen. W1N5 similarly could have either one O and one N or two N's in axial orientations, whereas only the former is found.

A theoretical energy gap between the two possibilities where N could be forced into an axial site instead of the preferred O is not available from these calculations. However, the energetic preference for water in the axial site may also be observed in the comparison between geometric isomers. Thus, low spin trans W2N4 is about 29 kJ/mol lower in energy than low spin cis W2N4, and low spin mer W3N3 is about 25 kJ/mol lower in energy than low spin fac W3N3. Finally, both cis and trans W4N2 isomers have O in trans positions, and there is no difference between the low spin isomer values. The preference for axial O over N is consistent with the weaker H_2O donor in the antibonding axial site, thus destabilizing the molecule less than would be the case with a stronger donor, NH_3, in this same location.

B. High Spin Energies. If one looks to the assignments in Figure 6 for the $S = {}^3/_2$ cases to provide a basis for explaining the high spin isomer energy ordering, the conclusions are not as firm as in the low spin case. While in low spin complexes there is a clear preference for O in an axial orientation, in high spin Co^{2+}, N is found only in some of

(22) Crystal field splitting, Δ_o, is the difference between the e_g and the t_{2g} orbital energies for an octahedral transition metal complex. A larger Δ_o indicates a stronger ligand.

(23) Zhang, Y.; Li, J.; Xu, H.; Hou, H.; Nishiura, M.; Imamoto, T. *J. Mol. Struct.* **1999**, *510*, 191−6.

Table 9. Energy Difference between High and Low Spin, $\Delta E = E_{low} - E_{high}$[a]

	ΔE RODFT gas phase	ΔE UDFT gas phase	ΔE RODFT solvated single point[b]	ΔE RODFT solvated optimized[b]
W6	102.51	101.25	109.20	78.66
W5N1	76.57	77.40	62.34	56.48
W4N2trans	52.72	53.56	43.51	38.91
W4N2cis	39.33	22.18	25.10	38.87
W3N3mer	19.66	35.15	9.20	6.95
W3N3fac	65.69	68.62	49.79	48.53
W2N4trans	21.76	22.59	28.95	12.76
W2N4cis	50.21	51.46	28.87	35.27
W1N5	14.23	16.32	0.42	1.63
N6	43.10	45.19	29.29	28.87

[a] Energy differences in kJ. [b] Difference in solution phase energy, E_{soln}.

the axial positions. The d^7 high spin symmetry is close to octahedral, and "axial" ligands are forced closer to the metal center with much smaller differences between the axial and equatorial positions. An intuitive argument would be that this reduces the potential advantage of placing O in an axial orientation that is farther from the metal. Because the H_2O ligands have two lone pairs oriented in a plane perpendicular to the protons, they overlap poorly with the d_{z^2} orbitals that define the axial direction but do overlap with the d_{xz}, d_{xy}, or d_{yz} orbitals and destabilize the isomer through an $e_{\pi x}$ or $e_{\pi y}$ repulsive interaction.[24] In high spin, the O ligand destabilization is more severe because of shorter bond lengths. Thus, by default, the stronger NH_3 ligand should be preferable because the presence of H_2O in that position would raise the energy of the isomer. In high spin, axial assignments are ambiguous, and indeed, the Jahn−Teller distortion is reduced in favor of the trend toward octahedral symmetry. Therefore, NH_3 cannot be assigned as the axial ligand in every case. Inspection of the density orbitals shows that high spin W2N4trans, W4N2cis, and W3N3mer adopt O−O pairs for overlap with the d_{z^2} orbital in the lower energy (HOMO − 1) e_g orbital. For W3N3mer, the N−N ligand pair appears to have axial symmetry in the HOMO. W5N1 has a N−O pair as axial in the HOMO, but W1N5 has a N−N pair overlapping with d_{z^2} in the HOMO and with N−O in the HOMO − 1. Because axial assignments in high spin geometries are not always clear, it would be an oversimplification to assume that NH_3 is a preferred axial ligand; however, it is obvious that the dominance of the H_2O ligand as an axial ligand in high spin geometries is gone.

C. Energy Difference between High and Low Spin. The central objective in this investigation is to determine which spin state is lowest in energy for Co^{2+} and if the ligand set influences that energy difference. Table 9 shows the energy difference between high and low spin configurations for each model compound as the ligands change from H_2O to NH_3. Calculations were done at RODFT and UDFT and give almost identical results. In every case, the high spin configuration has the lower energy which would be anticipated given that H_2O and NH_3 are relatively weak field ligands. The difference is 59 kJ/mol lower for N6 than for W6 reflecting the greater ligand field strength of NH_3 which shifts the energy levels closer to the spin crossover point where the energy difference would be zero.

(24) Deeth, R. J. *Coord. Chem. Rev.* **2001**, *212*, 11−14.

Table 10. Energy Changes between Gas Phase and Continuum Solvent

	ΔE_{stab}[a] high spin kJ/mol	ΔE_{stab} low spin kJ/mol	ΔE_{reorg}[b] high spin kJ/mol	ΔE_{reorg} low spin kJ/mol
W6	852.78	901.07	63.64	20.33
W5N1	847.13	867.47	39.04	35.31
W4N2trans	838.14	849.94	57.99	18.24
W4N2cis	840.15	885.59	15.06	38.87
W3N3mer	826.01	838.85	29.79	30.50
W3N3fac	822.57	840.52	18.87	23.10
W2N4trans	813.12	821.40	23.10	2.43
W2N4cis	813.75	830.06	19.46	24.10
W1N5	801.78	814.21	13.68	19.71
N6	789.77	816.97	3.72	3.39

[a] $\Delta E_{stab} = E_{soln} - E_{gas}$; E_{gas} is the energy of the solute in the gas phase at the gas phase optimized geometry; E_{soln} is the solution phase energy; $E_{soln} = E_{totalqm} - (E_{electron-solv})/2 - (E_{nuclear-solv})/2 + E_{cavity}$. [b] $\Delta E_{reorg} = E_{solute} - E_{gas}$; E_{solute} is the energy of only the solute in solution at the solution optimized geometry.

As NH_3 replaces H_2O, the energy difference between high and low spin generally decreases but shows a complex dependency on the isomer configuration and stereochemistry. For W2N4, it is the stabilization of the low spin energy in the trans isomer that decreases the difference between high and low spin. For W4N2, it is the destabilization of the high spin energy for the cis isomer that decreases the energy difference in that case. The very large decrease in the spin state energy difference for W3N3mer is due to the combined effect of the stabilization of the low spin and destabilization of the high spin state.

D. Effect of Solvent. Significant changes occur in the relative energies and the optimized geometries of the model compounds for both high and low spin Co^{2+} when the system includes a high dielectric solvent environment like water. Table 10 shows the differences in energy (ΔE_{stab}) between the optimized gas phase structure and the structure optimized in a continuum solvent environment.

The most notable effect of solvent is that the low spin molecules are stabilized more than the high spin molecules by at least 12−17 kJ/mol. Progressing through the series, substituting H_2O ligands for NH_3, the stabilization due to solvent increases for both spin states. Because the effect of solvation is greater for low spin, it also significantly changes the relative energy difference between one pair of isomers as Figure 6 shows. The W4N2 cis and trans energy difference is reduced by 12 kJ/mol. Reorganization energy, the difference between the total solute energy and the gas phase energy, is a measure of the change in the electronic structure of the molecule when surrounded by solvent. Table 10 shows that there is a large amount of reorganization energy for both of these isomers in their high spin states. Continuum solvent tends to create the most change for molecules with polar groups so the greater response of solvent to the model compounds with more H_2O ligands is not surprising. Likewise, the greater stabilization of the low spin cases, where at least two bonds are more polar because of their enhanced bond lengths, is also to be expected. Table 9 lists the energy difference between high and low spin and shows

that the inclusion of solvent in the calculations reduces the differences. The single point calculations at the gas phase optimized geometries reduce the difference in almost every case, but when geometry is allowed to optimize, the difference decreases even more in many of the structures in this series. It should be noted that for W3N3mer and W1N5 the differences are small enough to be considered insignificant and a spin equilibrium is expected. The implication is that with the proper ligand environment and when it is surrounded by an appropriate polarizing medium, it should be possible for Co^{2+} to be more stable in the low spin state. Such a medium might be present in the active site of a metalloprotein system.

Part of the solvent stability may be attributed to the changes in the optimized geometry of the molecule. The changes in Co−ligand bond lengths from surrounding continuum solvent are small but notable. In Tables 6 and 7, the changes, $\Delta d = d(\mathrm{Co-L})_{gas} - d(\mathrm{Co-L})_{solv}$, are listed below the gas phase bond lengths. In low spin, the solvent environment allows W6 to optimize to D_{4h} symmetry instead of the D_{2h} symmetry seen in the gas phase. The experimental crystal structures (Table 5) are qualitatively in agreement with the D_{2h} symmetry, but differences between trans pairs are smaller than those from the low spin gas phase calculation, pushing the structure to almost D_{4h} symmetry. The arrangement of charge on the solvent cavity surface accommodates longer Co−O bond lengths in the axial direction, and this effect is also seen in W6, W1N5, and W2N4cis. Axial Co−N bonds, in contrast, remain the same or shorten. Equatorial Co−N bonds also mostly shorten. With a large number of H_2O ligands, hydrogen bond interactions are possible, and the gas phase H_2O ligands orient themselves favorably for these interactions. Such attractions can be softened by the solvent cavity.

Similar to the effect of solvent for low spin, in high spin, the axial bonds in W6 lengthen considerably. High spin W6 assumes D_{2h} symmetry in the solvent environment instead of D_{4h} seen in the gas phase. In W5N1, there is a lengthening of the axial Co−O bond but only a minor change in the Co−N axial bond. In N6, the molecule is mostly octahedral, but the Co−N bonds have decreased approximately 0.02 Å. Equatorial Co−N bonds shorten relative to their gas phase values as the number of H_2O ligands increases. The largest reorganization energy is found among those compounds with the most H_2O ligands, as would be expected from the more polar character of that group.

Conclusions

DFT calculations predict that six-coordinate Co^{2+} complexes of general formula $[Co(H_2O)_{6-n}(NH_3)_n]^{2+}$, $n = 0-6$, adopt a high spin state. The difference in spin states is larger for H_2O ligands and depends on the configuration and stereochemistry of NH_3 and H_2O ligands. The inclusion of continuum solvation changes the magnitude but not the quality of the results in that high spin is less than or equal to the low spin energy in all cases. Optimized geometries show that high spin is close to octahedral symmetry while low spin permits significant Jahn−Teller distortions. Axial positions are dominated by H_2O ligands in low spin cases consistent with H_2O being a weaker ligand than NH_3, which would exhibit a stronger destabilizing $p_\sigma-d_\pi$ interaction than H_2O. In high spin, a preference for axial NH_3 ligands can be identified in some of the structures suggesting that the shorter M−L distances now permit the destabilizing π interactions to dominate although the distinction between axial and equatorial is sometimes ambiguous. Orbital compositions confirm that the calculated geometries are consistent with NH_3 ligands dominated by σ interactions and H_2O perturbed by π interactions with Co d orbitals.

The introduction of solvent via a continuum solvent approximation causes significant change in the relative energies computed in the gas phase, preferentially stabilizing the low spin configurations. As a result, the spin state energy differences for both W3N3mer and W1N5 are predicted to be close to zero. The energy changes uncovered in these calculations thus suggest that a suitable environment, say, from a surrounding protein, coupled with the proper combination of ligands, could alter which spin state is most stable.

Acknowledgment. The authors would like to acknowledge the competent assistance of Anthony Ginnetti and helpful comments from Dennis Lichtenberger. R.J.D. acknowledges the Engineering and Physical Research council for the provision of computing facilities.

IC0257930